Coordination Chemistry Reviews
219–221 (2001) 99–123

COORDINATION
CHEMISTRY
REVIEWS

www.elsevier.com/locate/ccr

Optically active phthalocyanines

Nagao Kobayashi *

Department of Chemistry, Graduate School of Science, Tohoku University, Sendai 980-8578, Japan

Received 8 September 2000; accepted 19 December 2000

Contents

Abstract

Optically active phthalocyanines (Pcs) reported to date have been reviewed. These are classified into three groups: (i) Pcs containing chiral carbons in the side chain. This type of Pc is further divided into two groups, i.e. Pcs with eight long alkyl chains attached directly or indirectly onto the periphery of the Pc core, and Pcs linked with small cyclic compounds. The former always form liquid crystals; (ii) Pcs with optically active aromatic molecules. This group includes helicene and binaphthyl-substituted species; (iii) Pcs with planar asymmetry. Synthesis, characterization and some spectroscopic properties have been summarized, and an

---

* Tel./fax: +81-22-2177719.
E-mail address: nagaok@mail.cc.tohoku.ac.jp (N. Kobayashi).

PII: S0010-8545(01)00323-X

outlook for future chiral phthalocyanines given.

Keywords: Optically active; Phthalocyanine; Chiral; Synthesis; Property; Circular dichroism

---

1. Introduction

Optical activity is omnipresent in nature. In the case of porphyrinic compounds, hemoproteins and chlorophylls have been well known for many years. Synthetic chiral porphyrins have also been reported intensively during the last 20 years or so, but the history of optically active phthalocyanines (Pcs) is approximately half that of porphyrins. One of the reasons for this appears to be difficulty in controlling the molecular structures of Pcs, since they are generally obtained by template reactions. However, chiral Pcs are more attractive than chiral porphyrins in some respects. For example, since Pcs are prone to co-facial aggregation, they may stack one-dimensionally to form helical superstructures, and this has indeed been proven as shown in this manuscript. In addition, in order to analyze the generation mechanism of their circular dichroism (CD), Pcs are superior to porphyrins, since the Q band which corresponds to the longest allowed transition is much more intense. Thus, studies in these directions have been performed for chiral Pcs. In this review, the synthesis and some representative properties of hitherto reported chiral Pcs are described.

2. Phthalocyanines containing chiral carbons in the side chain

2.1. Long alkyl chain-substituted species

It has long been known that Pcs substituted with eight long alkyl-, alkoxymethyl- or alkoxy chains on their periphery display mesomorphic behavior [1–11]. In 1988, Cho and Lim introduced chiral carbon atoms in the long alkoxy chains of H_2- and CuPcs [5]. Starting from commercially available *S*-(+)-1,2-propanediol, the precursor phthalonitrile **1** was obtained in ca. 20% total yield (Scheme 1). Compound **1** was then tetracyclized by, what we term, an ‘isoindoline method’ [12] to produce H_2Pc, **2**H_2, in 34% yield. This compound and its copper derivative **2**Cu showed mesogenic behavior at 23–158 and 29–191°C, respectively.

The second example of this type of Pc is one containing eight (*S*)-3,7-dimethyloctoxy substituents (*S*)**3** [13,14] (Fig. 1(a)). The starting phthalonitrile, bis-4,5-{(*S*)3,7-dimethyloctoxy}-phthalonitrile, was prepared from (*S*)-citronellol [15]. The phase transition temperatures of chiral (*S*)**3** were measured and compared with those of racemic (*R*,*S*)**3**. (*R*,*S*)**3** showed a crystalline (*K*) to hexagonal columnar mesophase (D_h) transition at 70°C and a D_h to isotropic phase (*I*) transition at 295°C. While (*S*)**3** showed a much greater number of transitions: an amorphous to

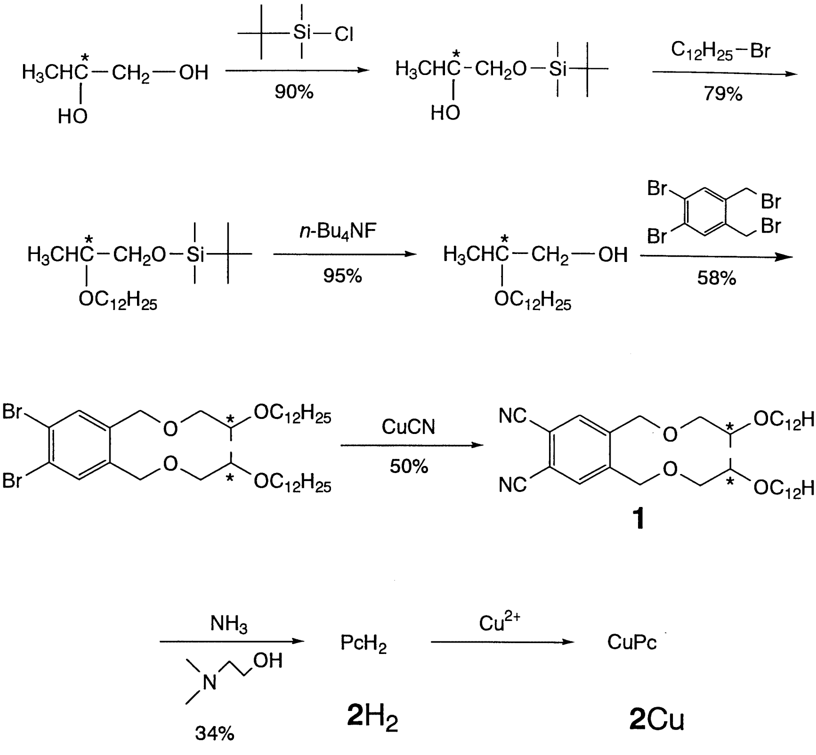

Scheme 1.

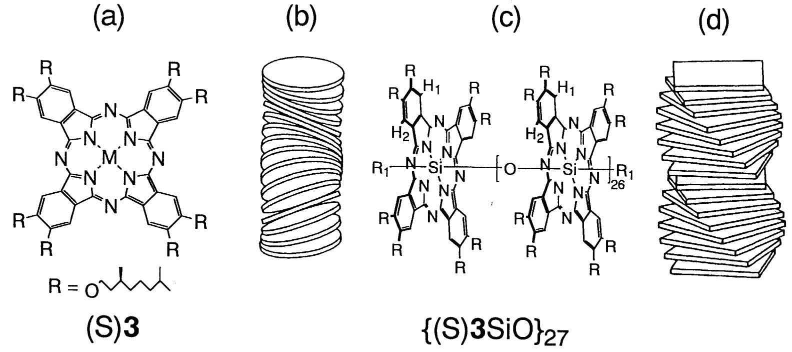

Fig. 1. Structues of (a) optically active Pc (*S*)**3** and (b) its proposed arrangement in mesophase (ovals represent Pc molecules); (c) μ-oxo oligomer of (*S*)**3**Si (polymerization degree = ca. 27), and (d) its proposed arrangement in mesophase (rectangles represent Pc plane).

chiral D_h phase (D_h^*) transition at 45–65°C; a transition between an unknown columnar mesophase (D) and D_h^* at 14°C; a transition between D_h^* and a rectangular columnar mesophase (D_r) at 111 (in heating runs) or 95–75°C (in cooling runs); and a transition between D_r and I at 295°C. When (*S*)**3** was slowly cooled down from the isotropic phase to the mesophase, a mozaic texture appeared which is characteristic of a discotic mesophase. However, when (*S*)**3** was quickly cooled down from the isotropic phase to room temperature, a texture with spiralized concentric rings was observed. From X-ray results which show reflections at 3.63, 3.43 and 3.22 Å, the mesophase of (*S*)**3** at 80°C was described as a D_h^* phase, in which a helical superstructure is present with a periodicity of about 55 Å (each period including about 16 Pc layers) (in contrast, this type of superstructure was not suggested for racemic (*R*,*S*)**3**). In a proposed structure (Fig. 1(b)), the Pc molecules are slightly tilted and the normal of the Pc planes rotates around the columnar axis.

When (*S*)**3** was transferred to a hydrophobic glass slide from the air–water interface by the LB technique (20 layers were deposited with X-type transfer), analysis suggested that they were oriented edge-on with respect to the water surface. This LB film showed a positive CD spectrum with a similar shape to the electronic absorption spectrum. Since a dilute chloroform solution of (*S*)**3** did not produce any CD activity, the authors claimed that the CD activity of the LB film must result from the chiral stacking.

Other interesting phenomena of (*S*)**3** and (*R*,*S*)**3** were found in their temperature-dependent emission spectra. The emission intensity of the both compounds was seen to decrease gradually with increasing temperature until a plateau was reached at approximately 200 K, which could be explained by the fact that excitons migrate faster through the stacks at higher temperatures. At around 345 K, the emission dropped to almost zero. In the case of racemic (*R*,*S*)**3**, this sudden change in intensity coincided with the $K \rightarrow D_h$ transition, but for the chiral (*S*)**3** the disappearance of the emission was suggested to be related to the transformation of a distorted columnar mesophase to an undisordered one. With decreasing temperature from 363 to 4 K, the emission maximum wavelength of (*S*)**3** was found to shift to shorter wavelength, while that of (*R*,*S*)**3** shifted to longer wavelength. This contrasting behavior was explained by a change in the radiative decay mechanism, since the wavelengths of emission were reported to be at shorter wavelength for the intrinsic sites (positionally undisturbed Pc molecules, radiative decay) and at longer wavelength for the extrinsic sites (strongly disturbed Pc molecules, radiative decay) [16]. They conjectured that (*S*)**3** is more or less co-facially stacked at 4 K and therefore fast energy migration is still possible, but trapping takes place more frequently at the large number of distorted (extrinsic) sites. On increasing the temperature, thermal detrapping occurs, and emission from the undistorted (intrinsic) sites at shorter wavelength became predominant.

The dose-normalized end-of-pulse conductivity of (*R*,*S*)**3** and (*S*)**3** is also compared. A sudden decrease of the conductivity by a factor of five at the $K \rightarrow D_h$ transition was observed for (*R*,*S*)**3**, while (*S*)**3** did not show such a sudden decrease, in agreement with the absence of a $K \rightarrow D_h$ transition. Remarkably, the

$D_h^* \rightarrow D_r$ transition at 111°C had no influence on the charge migration. The conductivity measurements corroborate the idea that the irreversible endothermic peak observed by DSC between 45 and 65°C is not a real phase transition but a slow reorganization of (*S*)**3** molecules.

The isoindoline derivative of (*S*,*S*)-1,2-dicyano-4,5-bis(3,7-dimethyloctoxy)-benzene and $SiCl_4$ was reacted in quinoline at 190°C, and the two axial Cl groups of the resultant Pc hydrolyzed to produce (*S*)**3**$Si(OH)_2$. Dehydration of this Pc at 200°C in vacuo produced its μ-oxo polymer with a polymerization degree of ca. 27, $\{(S)\mathbf{3}SiO\}_{27}$ (Fig. 1(c)) [17]. For this polymer, a helical arrangement represented in Fig. 1(d) was proposed, since the interplanar distance in μ-oxo SiPc is thought to be only 3.3 Å [18]. From the CD pattern corresponding to the main Q band, this polymer was suggested to be in the form of a left-handed helix.

The next examples of this type of Pc are those shown in Fig. 2 [19]. As seen in this figure, Pcs (S)**4** and its polymer $\{(S)\mathbf{4}SiO\}_n$ are similar in structure to (*S*)**3** and $\{(S)\mathbf{3}SiO\}_{27}$ above, respectively, except that crown ether units are introduced between the Pc core and chiral long alkoxy chains. Scheme 2 shows the synthetic pathways leading to the phthalonitrile precursors, **5**, used for the synthesis of (*S*)**4**, together with conditions and yields. After a nine-step reaction starting from catechol, **5** was obtained in 4.1% total yield, and by refluxing its isoindoline derivative in *N*,*N*-dimethylethanol, (*S*)**4** was obtained in 20% yield. The overall diameter of (*S*)**4** with extended tails is 60 Å and its thickness is 3.4 Å. When (*S*)**4** was heated in an organic solvent such as chloroform, at concentrations higher than 5 mg ml^{-1}, and then cooled slowly, strong aggregation to an organogel took place. Electron micrographs showed that the gel was composed of long, left-handedly twisted fibers, which have nanometer diameter and micrometer length. The bundles typically contained up to 25 fibers, each with the diameter of one single (*S*)**4** molecule (60 Å).

At ca. 10 μM concentrations, (*S*)**4** showed no aggregation in chloroform, but in 1:1 v/v chloroform:methanol, the main Q band shifted from ca. 700 to 600 nm, indicating co-facial aggregation. Corresponding to this Q band, the CD spectrum showed a plus-to-minus pattern when viewing from longer wavelength, suggesting the presence of a right-handed helical arrangement of the transition dipoles of the Pcs within a stack of Pc molecules in an aggregate. Polymer $\{(S)\mathbf{4}SiO\}_n$, obtained in vacuo at ca. 200°C, showed, in chloroform, a similar CD curve to (*S*)**4** in 1:1 v/v chloroform:methanol, indicative of a right-handed helical structure. Taking into account again that the interplanar distance of Pcs in μ-oxo SiPc is short (3.3 Å) [18], a columnar structure, drawn as Fig. 1(d) was proposed for $\{(S)\mathbf{4}SiO\}_n$.

A fiber with a right-handed twist and the structure of Fig. 1(d), such as organogel of (*S*)**4**, has a 'grooved' exterior. In order to maximize the van der Waals contact between two fibers twisted around each other, each of them has to bend over in order to fit into the groove of the other fiber. From the tilting angle between the two fibers measured in electron micrographs (125°), the staggering angle between two monomers was estimated theoretically to be 12°, in consideration of the diameter of (*S*)**4** (60 Å) and the interplanar stacking distance of 3.4 Å. In addition, for (*S*)**4**, it was derived theoretically that for staggering angles larger than 6.5°, a

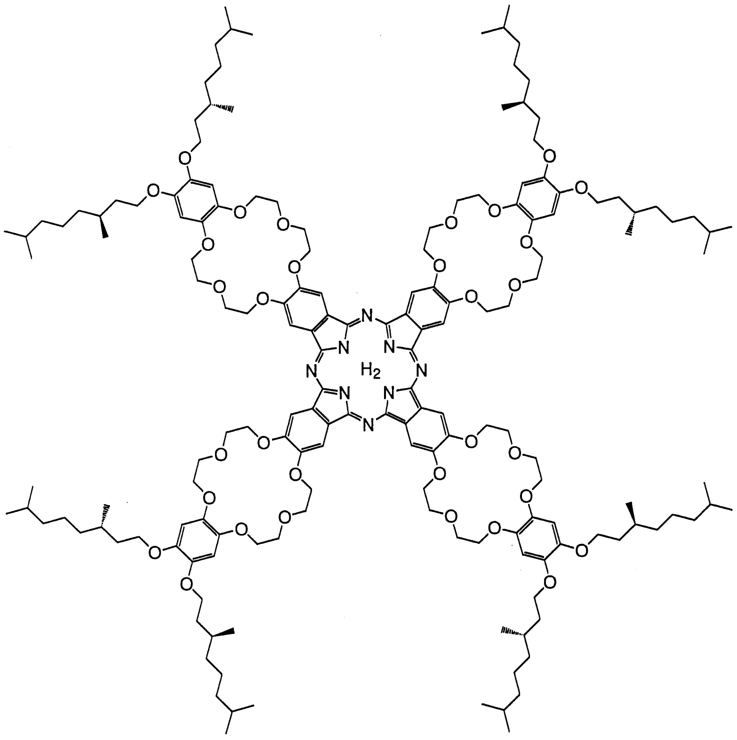

(S)4

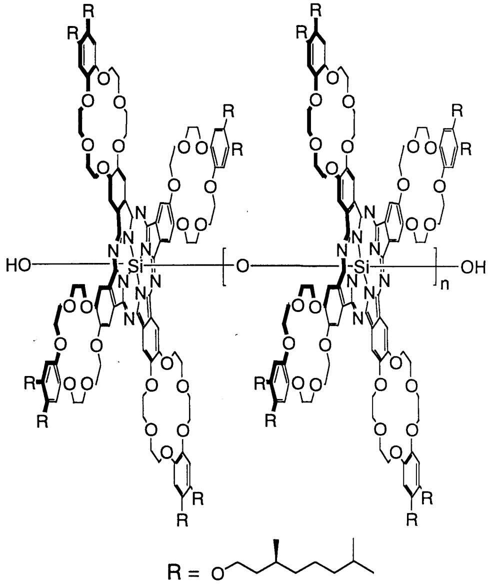

{(S)4SiO}$_{27}$

Fig. 2. Structures of optically active Pc (*S*)**4** and its μ-oxo SiPc polymer.

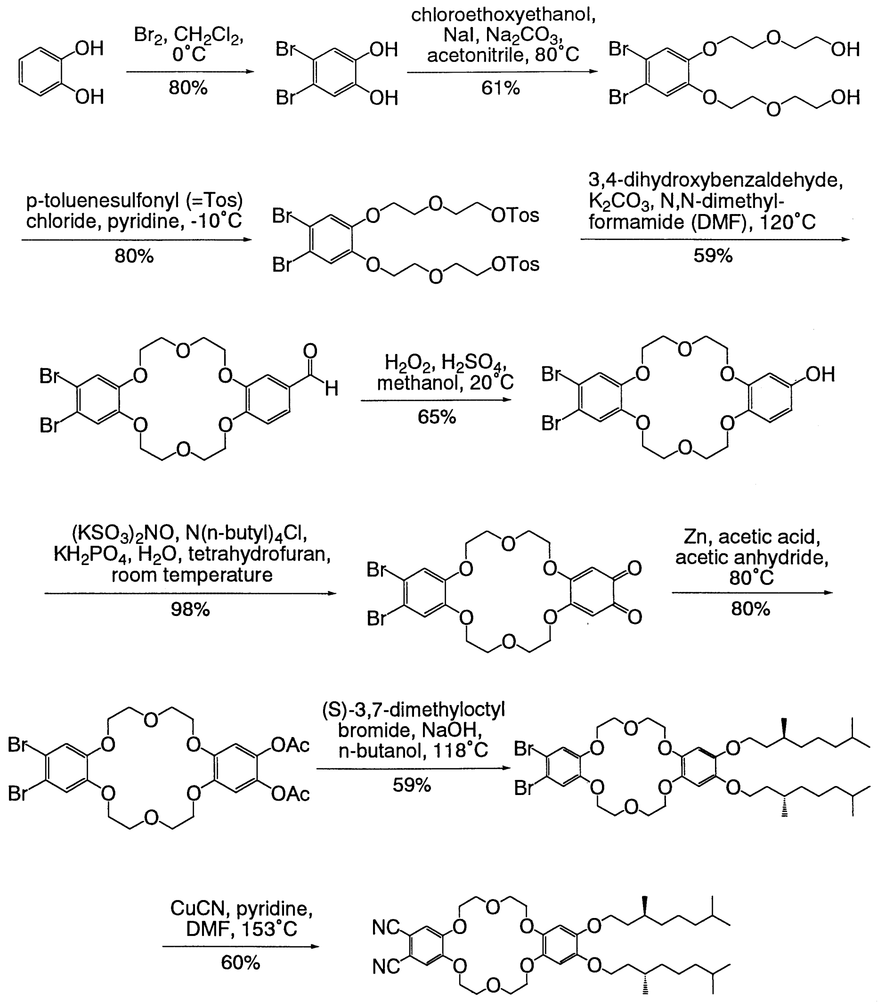

5

Scheme 2.

supercoiled structure is formed that has a helical sense opposite to that of the original helix.

Thus, experiments in [19] indicated that chiral information is transferred from the (*S*)-chiral centers in the tails of (*S*)**4** to the cores, where it is amplified to give right-handed helical fibers, which then further pack into left-handed supercoils. This supercoil structure was lost when K^+ ions were added, since the staggered conformation of Pc discs was forced into an eclipsed one.

The last Pc example grouped into this category is an amphiphilic CuPc, (*S*)**6**, prepared by the pathway shown in Scheme 3 [20]. In this scheme, the reaction of

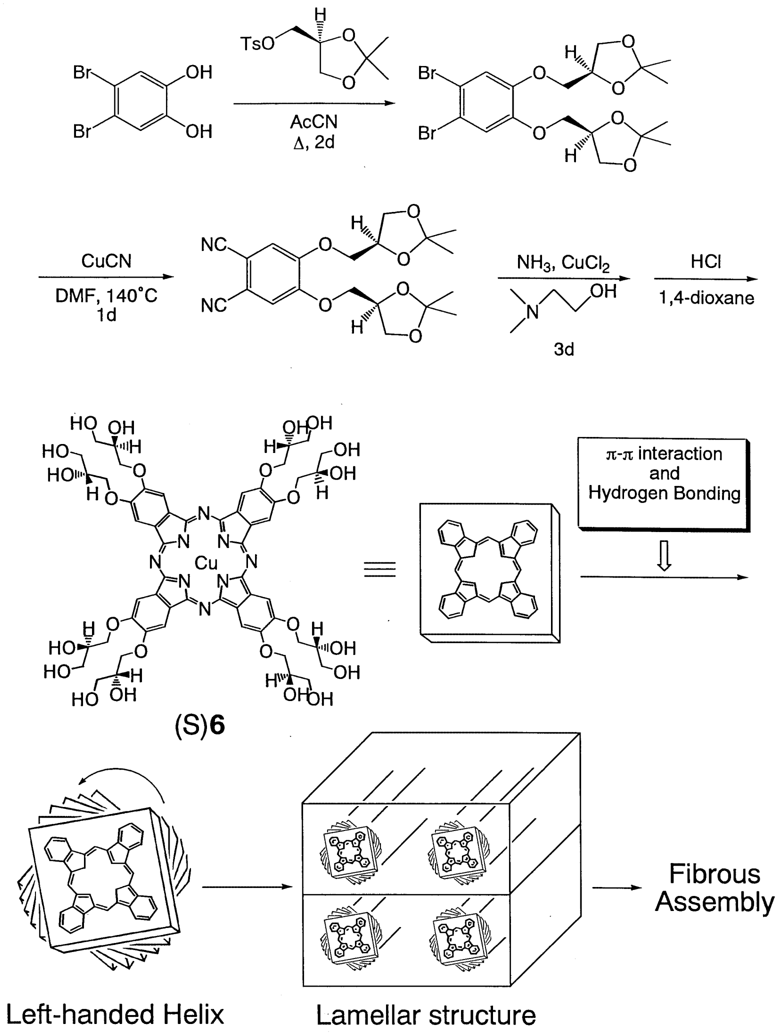

Scheme 3.

4,5-dibromocatechol and 2,2-dimethyl-1,3-dioxolan-4-ylmethyl *p*-toluenesulfonate was carried out in refluxing acetonitrile for 2 days. Deprotection of the protective group with HCl gave (*S*)**6** containing sixteen diol units. (*S*)**6** showed an absorption spectrum typical of nonaggregated Pc in DMSO. By admixing water, the spectrum changed to that of a co-facially aggregated Pc, with concomitant increase in specific viscosity. Although a solution of (*S*)**6** in DMSO was CD-inactive, the aqueous solution displayed CD activity. From the CD pattern in the Q band, which changes from negative to positive, viewing from the longer wavelength side, the Pc rings were suggested to be arranged in a left-handed helix. Since the racemic **6** did not show any CD activity in aqueous solution, the helical arrangement of the Pc rings was considered to result from the regularity of the hydrogen-bonding direction in (*S*)**6**. The morphology of the aggregate was examined by TEM. Samples were prepared by casting thin films of (*S*)**6** from aqueous solution onto a carbon-coated grid. The fibrous aggregates were observed with 10–40 nm widths, where (*S*)**6** gave thinner fibers compared to racemic **6**. This width implied that the fibrous aggregates were made up of an assembly of numerous Pc stacks.

2.2. Small ring-substituted species

Hoffman et al. reported the first synthesis of porphyrazinoctanol derivatives — the enantiometically pure, 'winged' spirane porphyrazines [21] — through the use of a simple, reliable strategy based on the Ley dispoke protection procedure [22]. Reaction of excess L-(+)-dimethyl tartrate **7** with 3,3′,4,4′-tetrahydro-6,6′-bi-*2H*-pyran in diethyl ether in the presence of hydrogen chloride gave only one diastereoisomer of the dispiroketal **8** in a 60% yield (Scheme 4). Monoiodination, followed by base-mediated *anti*-dehydroiodination, afforded chiral alkene **9** (53%). Amide formation in methanol at room temperature and dehydration with trifluoroacetic anhydride gave the starting dinitrile **10** in 77% overall yield, which was then cyclized in the presence of magnesium to the desired porphyrazine **11** in 45% yield. After demetalation of **11** in acetic acid at room temperature (78%), the metal-free derivative was analyzed by X-ray crystallography. The molecule had non-crystallographic D_2 symmetry. Other spectroscopic properties related to chirality were, unfortunately, not reported. However, it was reported that the ease of reduction of the differently functionalized porphyrazines follows the order: S-alkyl, O-alkyl, alkyl, and N-alkyl (the latter is more negative).

The second examples of this type of Pc derivatives are tetrapyrazinoporphyrazines containing four (1*R*)-(−)- or (1*S*)-(+)-camphor units [23]. The starting dinitriles, **12**, were obtained by condensing diaminomaleonitrile with (1*R*)-(−)- or (1*S*)-(+)-camphorquinone in refluxing ethanol containing a catalytic amount of concentrated hydrochloric acid in ca. 70–85% yields (Fig. 3, left). Cyclization of (*R*)**12** or (*S*)**12** in the presence of 1,8-diazabicyclo[5,4,0]-7-undecene (DBU) in dry ethanol gave metal-free (*R*)**13**H_2 and (*S*)**13**H_2 in ca. 33–40% yields. The corresponding copper complexes, (*R*)**13**Cu and (*S*)**13**Cu, were obtained in ca. 20% yield by reacting (*R*)**12** or (*S*)**12** in the presence of a copper salt and DBU. Fig. 3, right shows the electronic absorption and CD spectra of these species. The absorption spectra of **13**H_2 and **13**Cu are typical of those of metal-free and metalloPcs [24], although the Q band lies at slightly shorter wavelength than those of the normal Pcs [25,26]. As stated above for (*S*)**3** and (*S*)**4**, the CD intensity in this type of species is very weak, since the perturbation by optically active carbons in the side chain on the Pc chromophore is small. However, accummulation of measurements and subsequent smoothing procedure enabled us to obtain firm spectra, shown in Fig. 3, right. The shape of the CD spectra of (*R*)**13**H_2 and (*S*)**13**H_2 is similar to that of the absorption spectra, although the signs were positive and negative through all regions for (*R*)**13**H_2 and (*S*)**13**H_2, respectively. From the result which is described

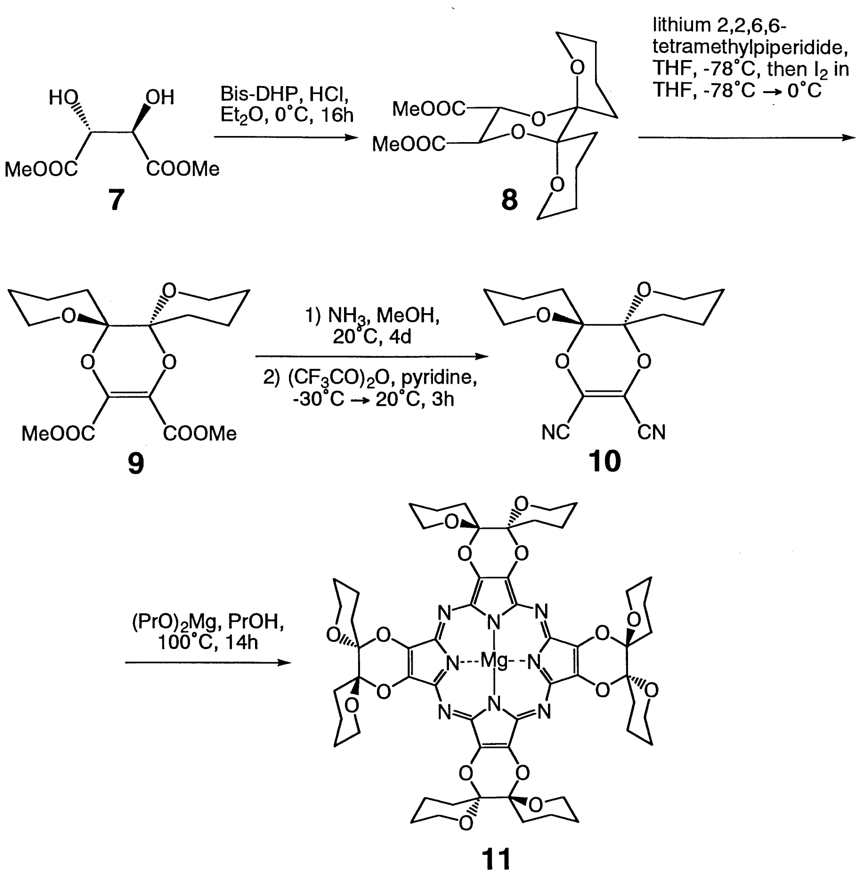

Scheme 4.

in the following section [27], it was concluded that the chiral carbons in (*R*)**13**H_2 and (*S*)**13**H_2 gave asymmetric fields of left- and right-handed conformers, respectively. (*R*)**13**Cu and (*S*)**13**Cu showed a similar type of CD behavior, although they gave CDs of opposite signs of comperative intensity corresponding to the Q_{00} absorption band. Since the strict molecular symmetry of (*R*)**13**Cu and (*S*)**13**Cu is lower than D_{4h}, and considering that the apparently single Q_{00} band is the result of superimposition of closely spaced Qx and Qy bands, it was tentatively conjectured that the asymmetric interaction between the chiral center in the peripheral substituents and the Qx and Qy transitions induced CD of opposite signs. However, the detailed CD generation mechanism for this phenomenon is still unknown.

(*R*)**13**Cu and (*S*)**13**Cu form co-facial dimers in a mixture of 1:1:2 v/v/v dioxane:*tert*-buthyl alcohol:water. Under this condition, the sign of the CD spectrum of (*R*)**13**Cu changed from negative to positive in both the Q and Soret band regions on going from longer to shorter wavelength, while that of (*S*)**13**Cu altered in the opposite manner. These changes in CD sign indicated that (*R*)**13**Cu and (*S*)**13**Cu have opposite chirality of stacking, left-handed for the former and right-handed for the latter. Thus, control of chirality of stacking was attained by changing the configuration of the carbon atoms in the substituents.

3. Phthalocyanines with optically active aromatic molecules

3.1. Peripheral substitution

Chiral aromatic molecules can give strong asymmetric perturbation to the Pc chromophore through dipole–dipole interaction, thus providing an opportunity to study, for example, the CD generation mechanism. A chiral binaphthyl unit was first introduced through alkyl chains linked to the fourth and fifth positions of 1,2-dibromobenzene, **14** (Scheme 5) [27]. This compound was then heated in the presence of CuCN in DMF at 95–100°C to produce four binaphthyl-substituted **15** in ca. 4–5% yield. In a different approach, compounds **16** which have two ethanol units, were reacted with 4-nitrophthalonitrile to produce **17** containing two ph-

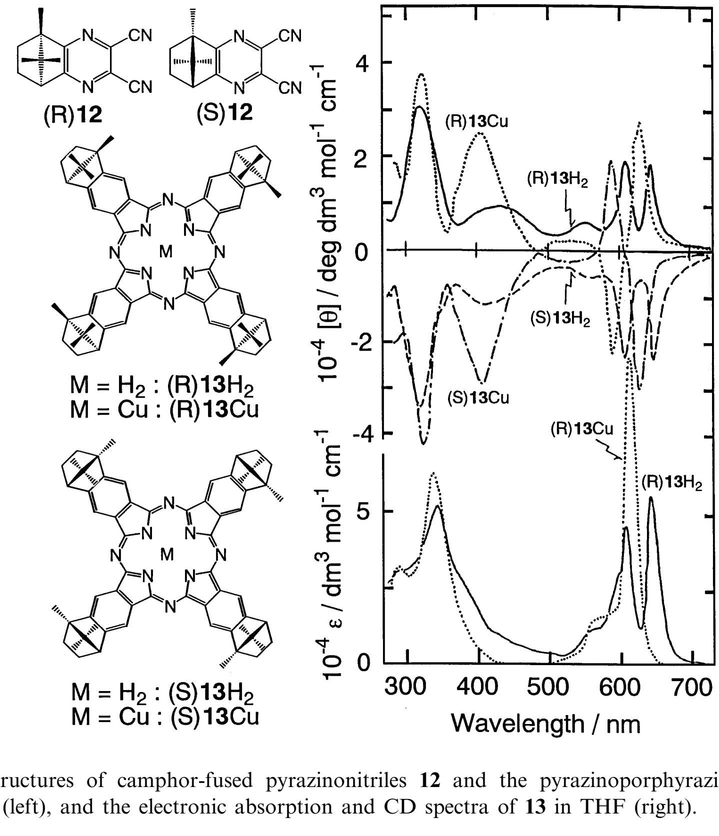

Fig. 3. Structures of camphor-fused pyrazinonitriles **12** and the pyrazinoporphyrazines **13** derived therefrom (left), and the electronic absorption and CD spectra of **13** in THF (right).

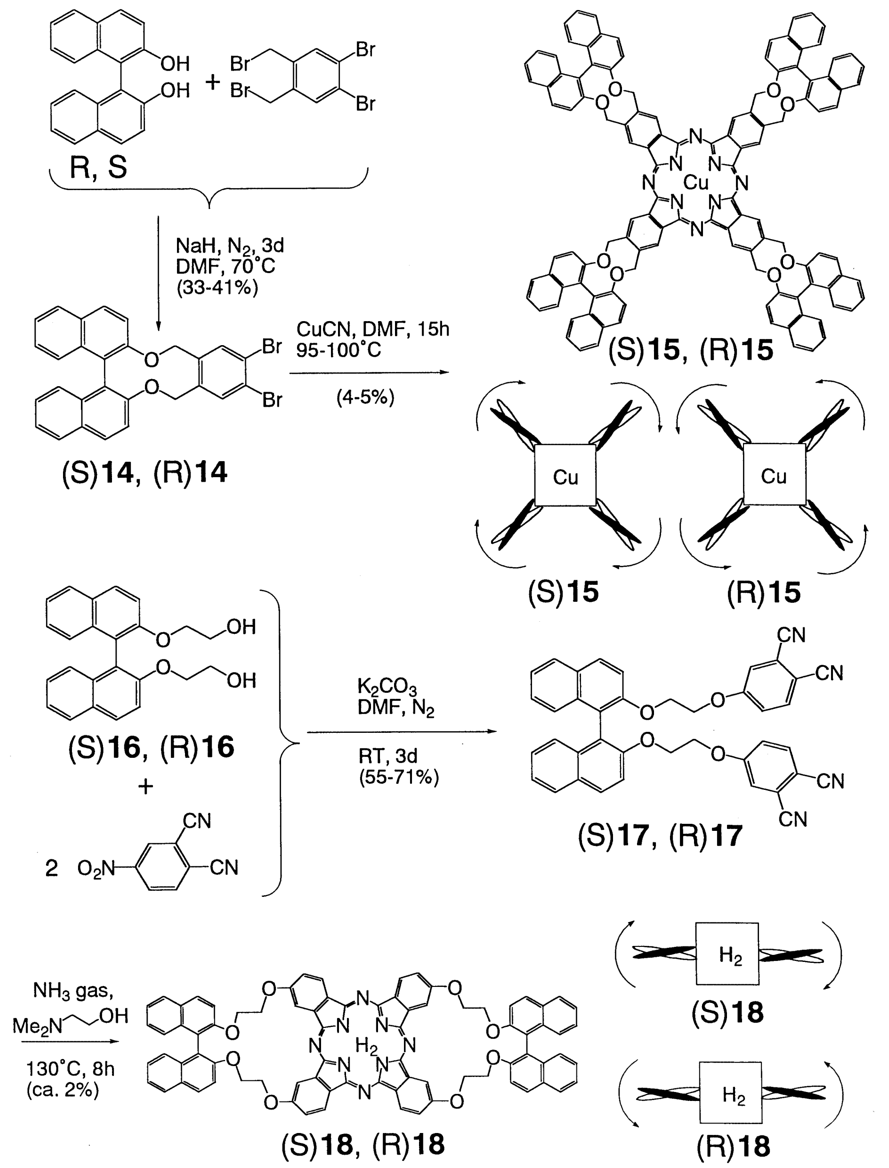

Scheme 5.

thalonitrile moieties in reasonable yields. This compound was refluxed in *N*,*N*-dimethylaminoalcohol while bubbling ammonia gas, to produce, after chromatography, two binaphthyl-linked Pc, **18**, in only 2% yield. Pcs containing (*R*)-(+)- and (*S*)-(−)-1,1′-binaphthyl units yielded positive and negative CD, respectively, throughout the entire absorption region of the Pc chlomophore. Since

(*R*)-(+)- and (*S*)-(−)-1,1′-binaphthyls were known to be left- and right-handed conformers, respectively [28], the results were taken to be an indication that negative CD is induced in the field of the right-handed conformer, while positive CD is generated in the field of the left-handed conformer [29]. When concentrations of Pcs were increased, monomer to co-facial dimer transformation was suggested spectroscopically. Interestingly, under dimer formation conditions, (*R*)**18** showed a negative-to-positive CD pattern at the main Q band, viewing from the longer wavelength, while (*S*)**18** showed the opposite pattern. Thus chirality control of the Pc stacking was achieved by introducing optically active conformers as substituent groups.

Since the yields of Pcs **15** and **18** were low, a new approach was attempted to prepare a reasonable amount of chiral Pcs of similar structure. The first step was the preparation of stable precursors. In this respect, compounds **19** (Fig. 4) were synthesized via a single-step high yielding reaction (over 90%) from commercially available (*S*)-(−)- or (*R*)-(+)-2,2′-dihydroxy-1,1′-binaphthyl and 3-nitrophthalonitrile without optical loss [30]. The most important property of these compounds is that they do not racemize under general Pc synthesis conditions because of the large steric hindrance due to the two bulky dicyanophenoxy groups, and of course no opposite isomer was produced when used for Pc synthesis. In addition, since the distance between the two phenoxy groups is close to the minimum required to link two adjacent benzene rings of Pc, the formation of oligomeric Pcs was suppressed. Thus, when the isoindoline derivatives of **19** were refluxed in *N*,*N*-dimethylaminoethanol for 3 h, Pcs **20** were obtained in more than

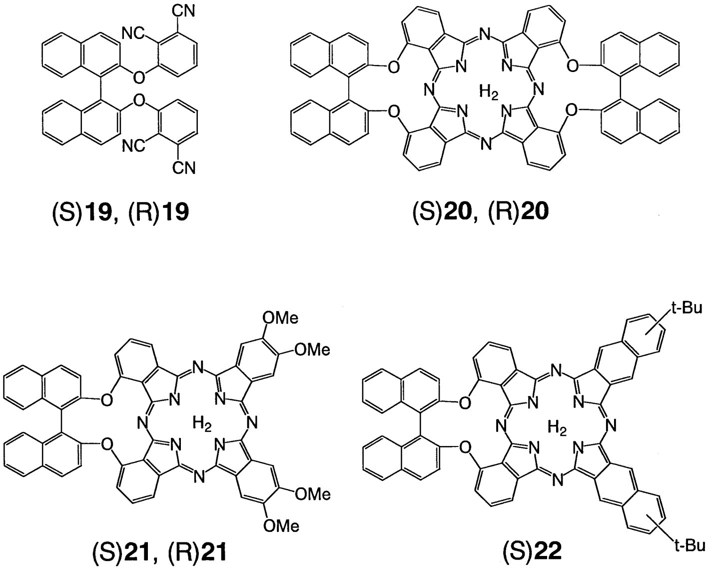

(S)**19**, (R)**19**

(S)**20**, (R)**20**

(S)**21**, (R)**21**

(S)**22**

Fig. 4. Optically active binaphthyl-linked bisphthalonitrile **19** and Pc derivatives derived therefrom.

30% yield. When the second isoindoline derivatives such as those derived from 4,5-dimethoxyphthalonitrile or 6-*tert*-butyl-2,3-naphthalonitrile were mixed, non-centrosymmetrically substituted Pcs **21** and **22** were obtained in more than 20% and ca. 10% yields, respectively, after chromatography. Although the solvent effect was discernible in the absorption and magnetic circular dichroism (MCD) spectra of Pcs **21** and **22**, it was most clearly seen in the CD spectra, reflecting perhaps a difference of aggregation trend.

In order to shorten the distance between the Pc core and binaphthyl units in compounds **15** for spectroscopic purposes, another phthalonitrile presursor, **23**, was prepared by the route shown in Scheme 6. The preparation of optically pure 1,1′-binaphthalene-2,2′-dithiol had been reported elsewhere [31]. Reaction of this dithiol with an equimolar amount of 4,5-dichlorophthalonitrile in the presence of K_2CO_3 in dry DMF at 70°C for 4 days under nitrogen gave **23** in 54% yield [32]. Tetracyclization of **23** was performed in the presence of lithium in refluxing hexanol for 1 h to yield a metal free Pc, **24**H_2, in 37% yield. Zinc insertion to **24**H_2 was carried out in 1:1 v/v ethanol:dichloroethane under reflux for 12 h while cobalt was inserted in DMF under reflux, to produce, respectively, **24**Zn and **24**Co.

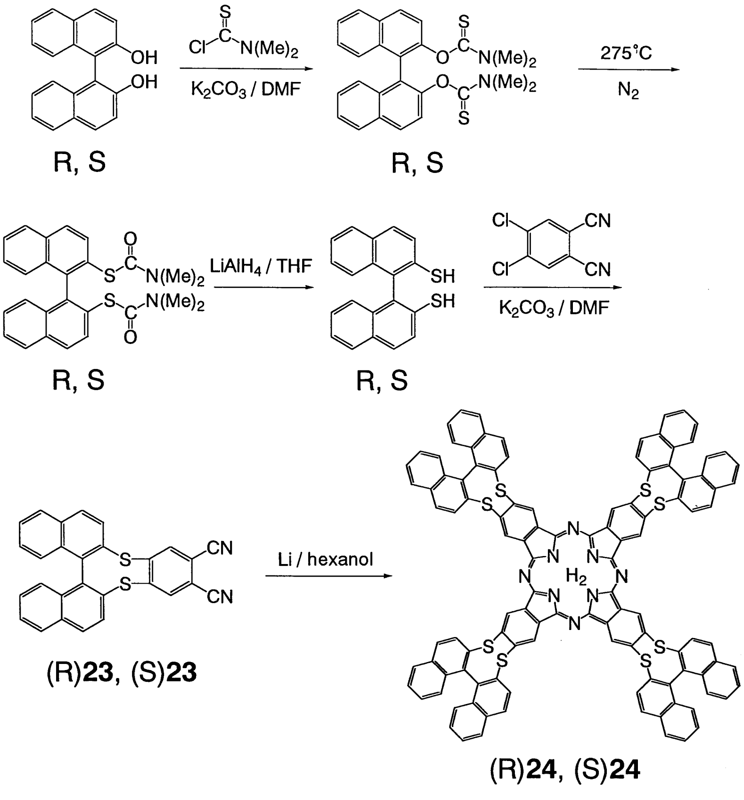

Scheme 6.

Fig. 5 shows the spectra of (*S*)- and (*R*)**24**Zn in THF. From the CD pattern in 200–270 nm, binaphthyl moiety retains right- and left helicity, respectively. In the absorption region of the Pc chromophore, (*R*)**24**Zn and (*S*)**24**Zn showed positive and negative CD, and although not shown here, all the (*R*)- and (*S*) binaphthyl-linked Pcs showed the same trend in sign. Apart from the sign, the shape of the CD spectra is similar to that of the absorption spectra for **24**H_2, **24**Zn and **24**Co, although the relative intensity of the Soret band to the Q band is larger in the CD spectra.

The induction mechanism for CD of compounds **20** and **24** were discussed. According to perturbation theory, two predominant mechanisms, termed the Kuhn–Kirkwood coupled oscillator mechanism and the CD stealing term, were taken into consideration. In the expression of the rotatory strength of the coupled oscillator mechanism, a term which is expressed by a vector product of the electric transition moment of the binaphthyl moiety and that of the Pc moiety appears, while in the CD stealing mechanism, the dot product of electric transition moment of the Pc moiety and the magnetic transition moment of the binaphthyl moiety

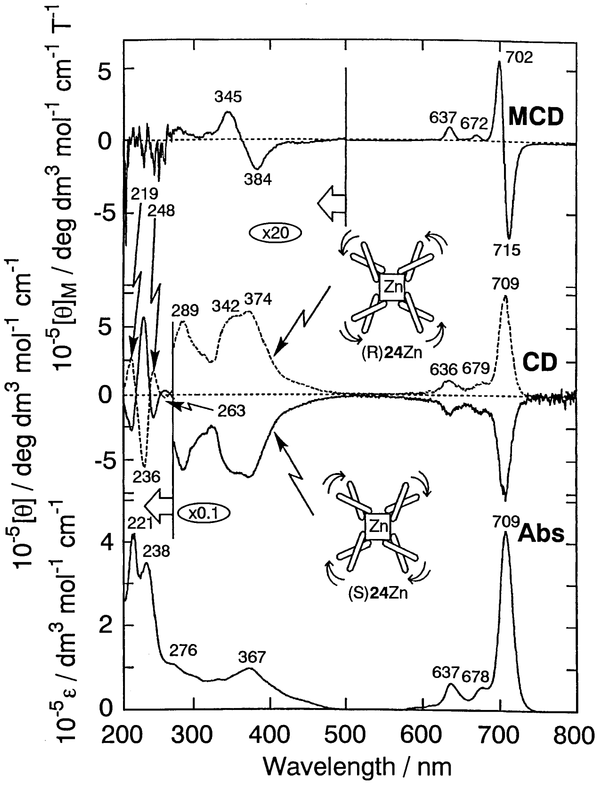

Fig. 5. Electronic absorption (bottom), CD (middle) and MCD (top) spectra of (*R*) and (*S*)**24**Zn in THF.

appears. Accordingly, all possible couplings were examined. The ratios which gives positive and negative rotational strengths (i.e. CD) were calculated for the structure of (*R*)**20** and (*R*)**24** (2.1 and 3.9, respectively). Thus, theoretical considerations have succeeded in producing the positive CD for (*R*)-binaphthyl-linked Pcs, in qualitative agreement with experiment. Of course, in the case of (*S*)-binapththyl-linked Pcs, negative rotatory strength was predominant, producing negative CD.

In the case of **20**, the shape of the electronic absorption and CD spectra was different, particularly in the Q band region (Fig. 6). The reason for this was also considered. From the shape of the electronic absorption spectrum in the Q band having a peak and shoulder, and the MCD spectrum having a trough and a peak corresponding to the absorption peak and shoulder, it was easily understood that the first excited state was not degenerate. After a theoretical consideration and molecular orbital calculations, it was found for (*R*)**20** that a large positive rotational strength lies at the absorption peak to the longer wavelength side while a small negative rotational strength locates at the absorption shoulder to shorter wavelength. Thus, these were the reasons that we observed a relatively sharp Q CD band compared with that of the Q absorption band (Fig. 6). In contrast, for **24**, the first excited state is degenerate (appearance of a symmetrical MCD band (Faraday *A* term) corresponding to the Q absorption peak). Accordingly, positive and negative rotational strength resided at the same wavelength, thereby producing CD curves similar in shape to the absorption spectra, apart from their magnitude.

The spectra of electrolyzed (*R*)**24**Co was recorded by applying a potential 720 mV negative of the first reduction (Fig. 7). With the progress of the electrolysis, the

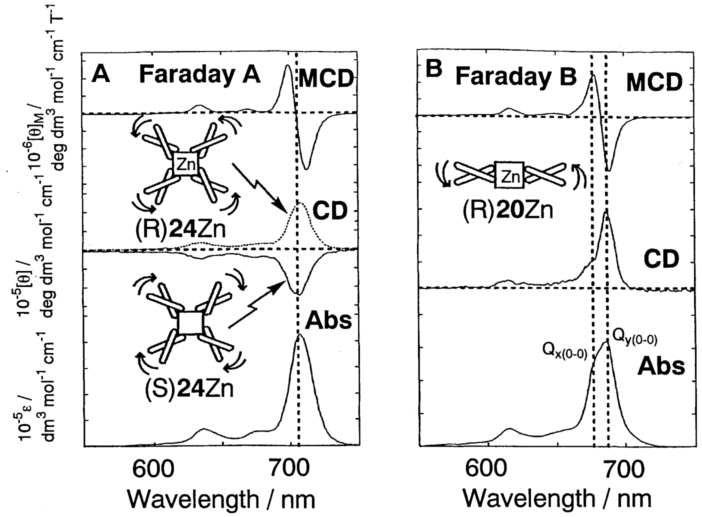

Fig. 6. Electronic absorption (bottom), CD (middle) and MCD (top) spectra of (*R*) and (*S*)**24**Zn (left) and (*R*)**20**Zn (right) in the Q band region in THF. The MCD and absorption spectra of **24**Zn indicate that the excited state of the Q band is degenerate, while those of (*R*)**20**Zn suggest it is not-degenerate.

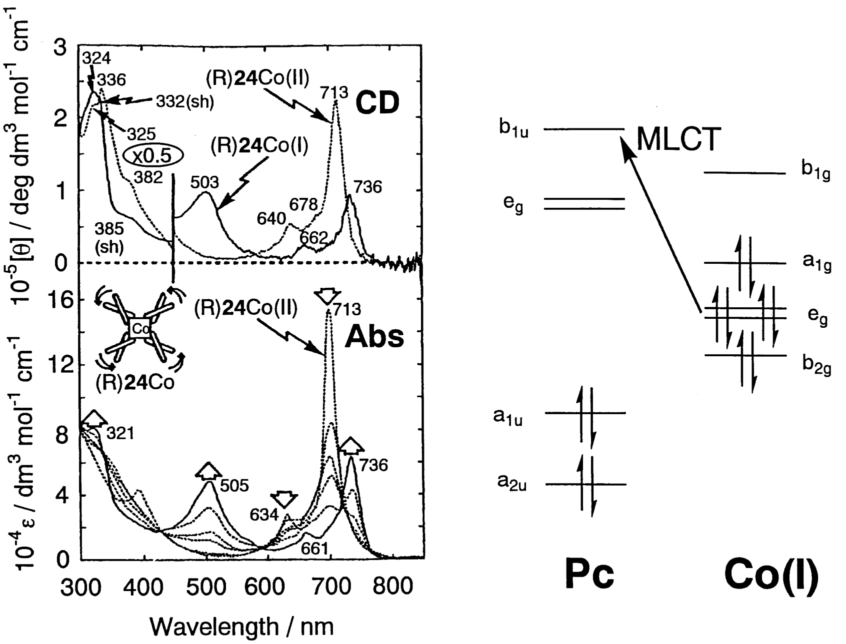

Fig. 7. Electronic absorption and CD spectra recorded during electrolysis of (*R*)**24**Co in *o*-dichlorobenzene (left). The initial species is in the Co(II) state, while the final species in the Co(I) state. Applied potential/V = − 1.00 V vs. Ag | AgCl. Supporting electrolyte was tetrabutylammoium perchlorate. The right-hand side is a schematic diagram of the highest occupied and lowest empty π orbitals of the Pc ring. Also included are the representations of a set of d-orbitals under D_4. The ordering of the latter is quite arbitrary.

Q band weakened and shifted to longer wavelength, and a new peak developed between the Soret and Q bands. This is a characteristic of the formation of a cobalt(I) species [33]. Both the starting Co(II) and reduced Co(I) species revealed positive CD spectra whose shapes were similar to those of the absorption spectra. The band between the Soret and Q bands has been assigned to an MLCT band from cobalt e_g to ligand b_{1u} orbital [34]. Accordingly, the symmetry of the first excited state is E_u as in the case of the Q ($a_{1u} \rightarrow e_g$) and the Soret states ($a_{2u} \rightarrow e_g$). Hence the fact that the CD sign of the MLCT band is positive, similarly to the Q and Soret bands, was taken as an indication that all these bands are in-plane polarized.

Fluorescence emission and excitation (Fig. 8, left) and even fluorescence-detected induced CD (FDICD) spectra (Fig. 8, right) were recorded for **24**H_2 and **24**Zn [35]. Both metal-free and zinc complexes showed at least S_1 and S_2 emissions. As for other Pcs reported to date [36–38], the Stokes shift of the S_1 emission is very small, while that of S_2 emission is large. The quantum yields (Φ_F) of S_1 emission is smaller compared to Pcs reported to date, since the Q bands of these compounds lie at longer wavelengths (nonradiative decay becomes easier with increasing wavelength).

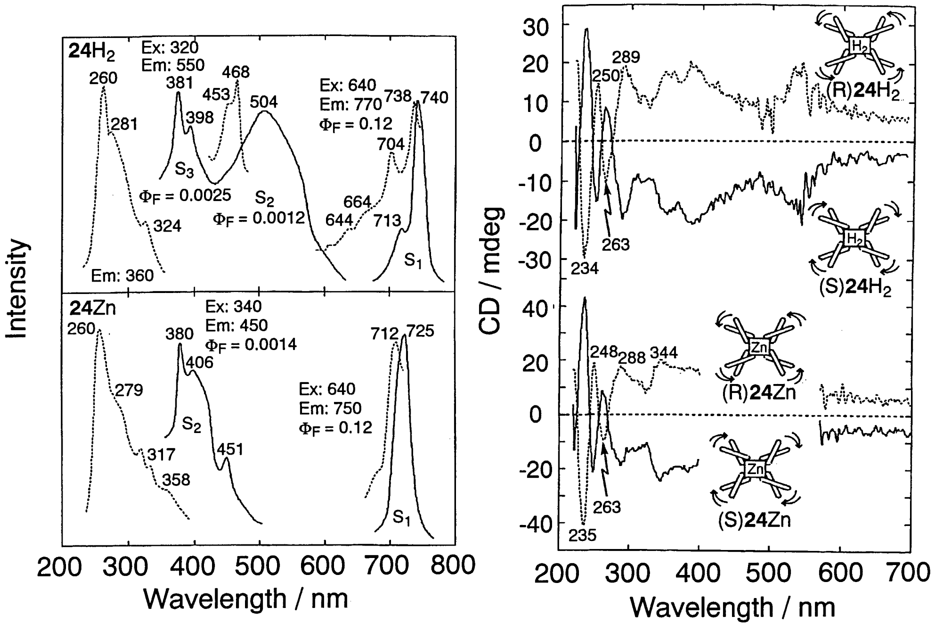

Fig. 8. Fluorescence emission and excitation spectra of **24**H_2 and **24**Zn in chloroform (left) and fluorescence detected induced CD (FDICD) spectra of the same compounds in THF (right). Excitation wavelengths, emission wavelengths used to record the excitation spectra, and quantum yields are indicated. The FDICD spectra of **24**Zn in 400–550 nm was not shown because of excessive noise. Concentrations of samples used for the measurements of FDICD were as follows: 5.30×10^{-6} mol l^{-1} for **24**H_2 and 1.34×10^{-6} mol l^{-1} for **24**Zn.

However, Φ_F values of S_2 emission were the largest among the Pcs known so far. The sign of the FDICD spectra of the S_1 emission was positive for the (*R*) species and negative for the (*S*) species, indicating that the (*R*) species absorbs left circularly polarized light more than the right, and vice versa for the (*S*) species.

Katz et al. recently reported a novel type of chiral Pc derivative, i.e. four nonracemic [7]helicene-fused pyrazinoporphyrazine, **25**, by the route shown in Scheme 7 [39]. The compound **26** in this Scheme was prepared in eight steps from 9,10-phenanthracenequinone [40]. The direct precursor **27** was then obtained in ca 50% yield via a four-step reaction from **26**. When **27** was refluxed with Cu or Ni salts in *N*,*N*-dimethylaminoethanol, its copper and nickel complexes, **25**Cu and **25**Ni, were obtained in 30 and 20% yields, respectively.

As for compounds **15**, **18**, and **24**, non-aggregated **25** with chromophores of (M)-helicity produced a positive CD sign associated with the Q_{00} band, and mainly a large negative sign in the Soret region. By changing the ratio of the solvent used for the measurements, the authors succeeded in recording the spectra, which may be assignable to aggregated species, i.e. the absorption spectra became broader and the absorption peak intensity weakened, but not shifted. Based on the PM3 calculations, the authors claimed that the molecules were separated co-facially by 3.4 Å, with one molecule rotated with respect to the other by 35°. However, this seems to be unusual phenomenon, since all co-facial dimers and oligomers of phthalocyanines and porphyrins reported to date showed the blue-shifted Q bands, if the distance is so short. In the aggregated state, the Q CD sign of (M) **25** changed from negative to positive, viewing from the longer wavelength side.

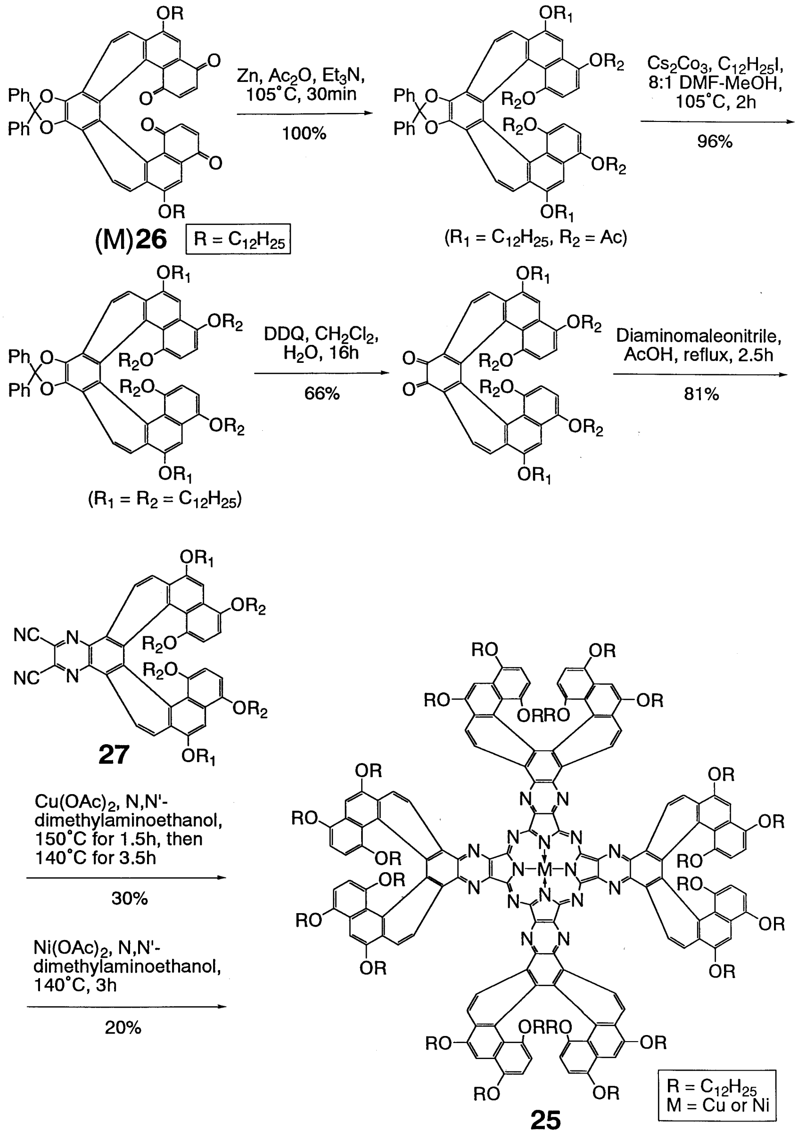

Scheme 7.

The beam of a Nd:YAG laser, initially polarized in the plane of incidence, was passed through a rotating quater waveplate and focused at an incident angle of 45° onto five-layer Langmuir–Blodgett (LB) films of **25** deposited on alkylsilanized glass, and the transmitted second-harmonic light was resolved into components polarized parallel and perpendicular to the plane of incidence. Assuming that the direction of the normal to the surface is that of the z-axis, four independent components of the second-order susceptibility tensor, χ_{xyz}, χ_{zxx}, χ_{xxz}, and χ_{zzz}, were evaluated. For the copper complex, these were 24, 3, 4, and 6 pm V^{-1} and for the nickel complex the values were 19, 4, 3, and 15 pm V^{-1} in the above order. For molecules having D_4 symmetry, such as **25**, the non-zero components of the molecular hyperpolarizability tensor are those associated with chirality [41], and these components can only contribute to chiral macroscopic susceptibility components. Since the analysis of the LB film indicated that compound **25** took an edge-on orientation, this meant only to χ_{xyz}, thereby explaining the largest magnitude among the four independent components of the tensor.

3.2. Axial substitution

By linking an optically active chromophore as an axial ligand, we can prepare Pcs with axial chirality. Utilyzing the reactivity of the axial oxygen in TiOPc, which is readily displayced by *ortho*-phenolic OH groups, with the elimination of water, to produce two ether linkages [42–44], *tert*-butylated TiOPc and (S)-(−)- or (R)-(+)-2,2′-dihydroxy-1,1′-binaphthyl were reacted in methylene chloride at room temperature for several hours. Purification using gel-permeation chromatography produced **28** in ca. 30% yield (Fig. 9) [45]. The Q_{00} band of their absorption spectra split into two peaks due to an exciton interaction of the Pc and binaphthyl ligands [43], while a very weak peak which has not been observed for general Pcs developped at ca. 510 nm (Fig. 10). In the CD spectrum, the (R)-binaphthyl-linked species showed a plus-to-minus pattern at the Q_{00} and the 510 nm bands, and a small negative-to-strong positive pattern in the Soret band region, viewing from

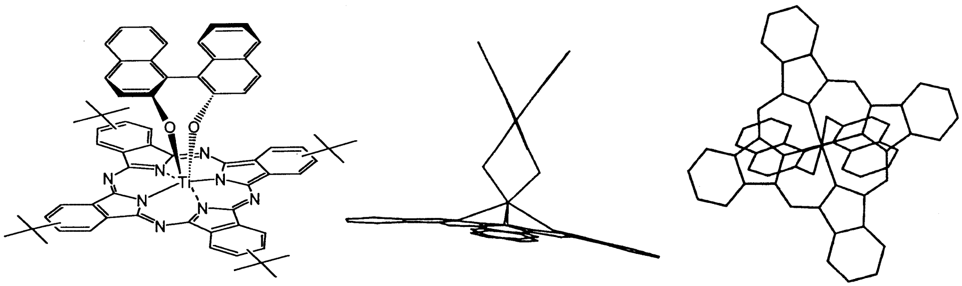

(S)28

Fig. 9. Structure of *tert*-butylated TiPc linked with a (S)-binaphthyl molecule as an axial ligand, **28** (left) and its optimized structures (middle and right) obtained using the PM3 Hamiltonian program.

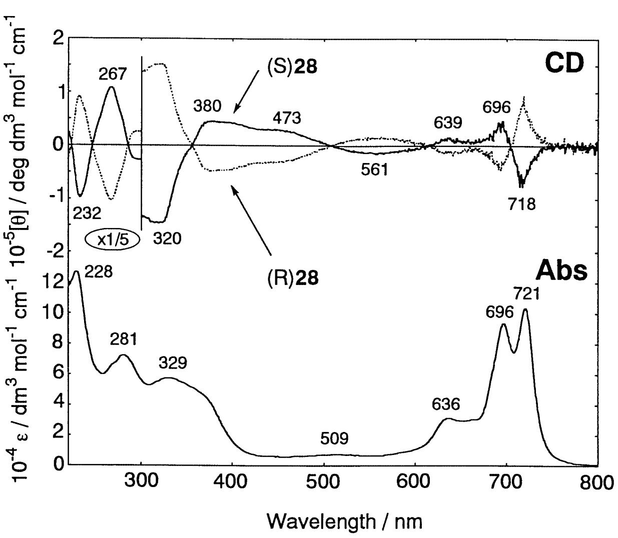

Fig. 10. Electronic absorption (bottom) and CD spectra (top) of **28** in THF.

longer wavelength side. If the Pc plane is completely planar, consideration of CD induction mechanisms using electronic dipole and magnetic dipole moments [32] suggests a positive sign at both the Soret and Q bands. However, since the optimized structure using the PM3 Hamiltonian program suggested an out-of-plane deviation of the Pc rings (Fig. 9, middle), the moment of this dirction may couple strongly with the long-axis polarized transitions of the binaphthyl unit, although it is uncertain at this stage whether this coupling would produce a positive or negative CD sign. The significantly deformed CD curves of the binaphthyl chromophore (ca. 200–280 nm) indeed suggest unignorable interaction between the Pc chromophore [46]. Concerning the 510 nm band, the molecular orbital calculations using a ZINDO/S Hamiltonian suggested a transition from the binaphthyl-centered HOMO-1 orbital to a titanium-centered orbital.

4. Phthalocyanines with planar asymmetry

4.1. Phthalocyanines

With the development of synthetic methods [47,48], it is now possible to prepare tetra-substituted MtPcs with single-handed rotation. If an axial ligand is attached from one side of the Pc plane, the resultant compound is a mixture of right-handed and left-handed conformers. VOPcs with single-handed rotation, **29**, were prepared in this way and resolved into two enantiomers by use of an optically active HPLC column (Fig. 11) [49]. Although both the electronic absorption and MCD spectra are those of MtPcs with D_{4h} symmetry [24], the two enantiomers showed CD of

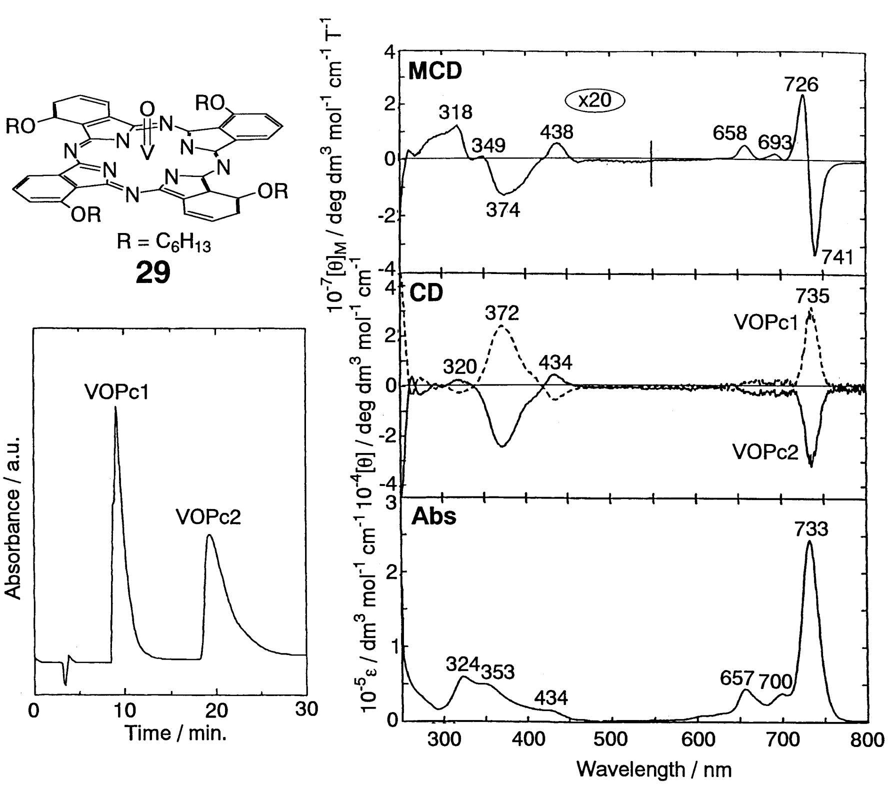

Fig. 11. Structure of a VOPc with single-handed rotation **29** (top left), and its HPLC chromatogram obtained using an inverse phase silica gel column coated with cellulose tris(3,5-dimethylphenylcarbamate) and mixtures of hexane and chloroform (bottom left). Their absorption, CD, and MCD spectra are shown on the right-hand side.

opposite signs. Interestingly, the sign at the π–π* transitions was opposte to that at the *n*–π* transition of ether oxygen in the substituents. Quantum chemical calculations suggested that the enantiomer showing a negative sign at the Q band was the left-handed conformer looking from the side of axial oxygen, while that giving a positive CD sign was the opposite right-handed conformer.

4.2. Subphthalocyanines

Subphthalocyanines (SubPcs) are composed of three isoindole units [50,51]. Accordingly, differing from tetra-substituted MtPcs which have four positional isomers, tri-substituted SubPcs (one group in each isoindole subunit) have only two positional isomers with C_1 and C_3 symmetry. These two constitutional isomers are each a mixture of two enantiomers. Therefore, it is potentially feasible to isolate these enantiomers [52,53]. Fig. 12 shows absorption and CD spectra of SubPc enantiomers with C_3 symmetry prepared from 5-*tert*-butyl-3-nitrophthalonitrile and

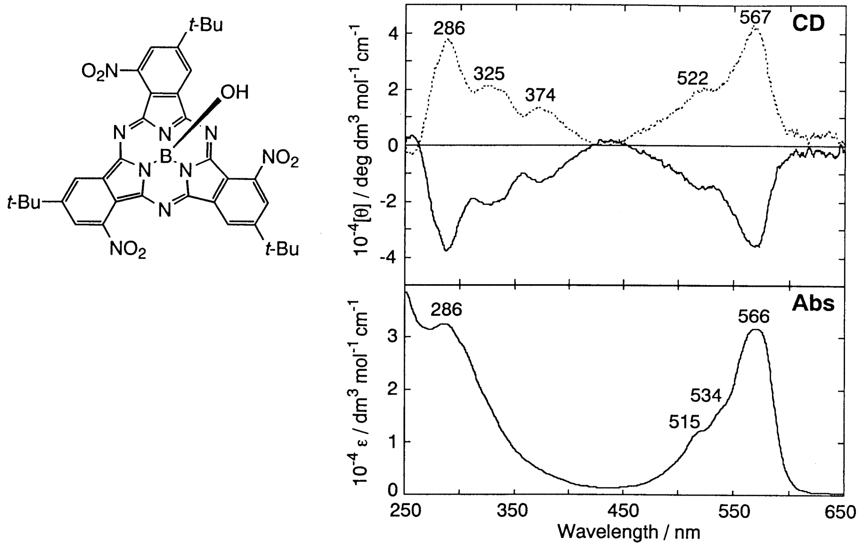

Fig. 12. Structure of a SubPc with C_3 symmetry obtained from 5-*tert*-butyl-3-nitrophthalonitrile (left) and the electronic absorption and CD spectra of the two enantiomers resolved therefrom (right). The same HPLC column used for Fig. 11 was used. The first eluting fragment gave negative CD and the second one positive CD sign.

BBr_3 [54]. Although the correlation between their CD sign and conformation is still unknown, the two enantiomers displayed a mirror-image relationship with respect to the intensity = 0 line. Compared with the above Pcs in Section 4.1, the CD intensity is larger for SubPc, since the SubPc plane is doming [51].

5. Conclusions and outlook

Chiral Pcs reported to date have been grouped into several classifications, and their synthesis and representative properties summarized. Since Pcs have been used intensively as industrial materials, there is good reason for further investigation of their solid state properties. As many of the representative monomeric chiral Pcs have already been reported, chiral Pcs consisting of pluralities of Pcs may become the next target. In the Pc chemistry, Pc analogues coordinated by metal-ligands such as those termed ‘Star-Porphyrazines’ are known to exist [55–57]. Pcs, which become optically active by the assistance or coordination of metals, may also be a new field yet to be elucidated.

Acknowledgements

This research was supported partly by the Ogasawara Science Foundation and a

Grant-in-Aid for Scientific Research (B) No. 11440192 from the Ministry of Education, Science, Sports, and Culture, Japan.

References

[1] C. Piechocki, J. Simon, A. Skoulios, D. Guillon, P. Weber, J. Am. Chem. Soc. 104 (1982) 5245.
[2] I. Cho, Y. Len, Chem. Lett. (1987) 2107.
[3] K. Ohta, L. Jacquemin, C. Sirlin, L. Bocio, J. Simon, New J. Chem. 12 (1988) 751.
[4] J.F. van der Pol, E. Neeleman, J.W. Zwikker, R.J.M. Nolte, W. Drenth, Recl. Trav. Chim. Pays-Bas 107 (1988) 615.
[5] I. Cho, Y. Lim, Mol. Cryst. Liq. Cryst. 154 (1988) 9.
[6] J.F. van der Pol, E. Neeleman, J.W. Zwikker, R.J.M. Nolte, W. Drenth, J. Aerts, R. Visser, S.J. Picken, Liq. Cryst. 6 (1989) 577.
[7] M.J. Cook, S.J. Cracknell, K.J. Harrison, J. Mater. Chem. 1 (1991) 703.
[8] A.N. Cammidge, M.J. Cook, K.J. Harrison, J. Chem. Soc. Perkin Trans (1991) 3053.
[9] P. Weber, D. Guillon, A. Scoulios, Liq. Cryst. 9 (1991) 3.
[10] M.K. Engel, P. Bassoul, L. Bocio, H. Lehmann, M. Hanack, J. Simon, Liq. Cryst. 15 (1993) 709.
[11] K. Ohta, S. Azumane, T. Watanabe, S. Tsukada, I. Yamamoto, Appl. Organomet. Chem. 10 (1996) 623 and Refs. [1–9] therein.
[12] P.J. Brach, S.J. Gramatica, O.A. Ossanna, L. Weinberger, J. Heterocycl. Chem. 7 (1970) 1403.
[13] C.F. van Nostrum, A.W. Bosman, G.H. Gelinck, S.J. Picken, P.G. Shouten, J.M. Warman, A.-J. Shouten, R.J.M. Nolte, J. Chem. Soc. Chem. Commun. (1993) 1120.
[14] C.F. van Nostrum, A.W. Bosman, G.H. Gelinck, P.G. Shouten, J.M. Warman, A.P.M. Kentgens, M.A.C. Devillers, A. Meijerink, S.J. Picken, U. Sohling, A.-J. Schouten, R.J.M. Nolte, Chem. Eur. J. 1 (1995) 171.
[15] (a) P.G. Shouten, J.F. van der Pol, J.W. Zwikker, W. Drenth, S.J. Picken, Mol. Cryst. Liq. Cryst. 195 (1991) 291. (b) P.G. Shouten, J.F. van der Pol, J.W. Zwikker, W. Drenth, S.J. Picken, Mol. Cryst. Liq. Cryst. 208 (1991) 109.
[16] G. Blasse, G.J. Dirksen, A. Meijerink, J.F. van der Pol, E. Neeleman, W. Drenth, Chem. Phys. Lett. 154 (1989) 420.
[17] H. Engelkamp, C.F. van Nostrum, S.J. Picken, R.J.M. Nolte, Chem. Commun. (1998) 979.
[18] D. Wohrle, in: C.C. Leznoff, A.B.P. Lever (Eds.), Phthalocyanines-Properties and Applications, vol. 1, VCH, New York, 1989, pp. 55–132.
[19] H. Engelkamp, S. Middlebeek, R.J.M. Nolte, Science 284 (1999) 785.
[20] M. Kimura, T. Muto, H. Takimoto, K. Wada, K. Ohta, K. Hanabusa, H. Shirai, N. Kobayashi, Langmuir 16 (2000) 2078.
[21] A.S. Cook, B.G. Williams, A.J.P. White, D.J. Williams, S.J. Lange, A.G.M. Barrett, B.M. Hoffman, Angew. Chem. Int. Ed. Engl. 36 (1997) 760.
[22] (a) S.V. Ley, M. Woods, A. Zanotti-Gerosa, Synthesis (1992) 52. (b) S.V. Ley, R. Leslie, P.D. Tiffin, M. Woods, Tet. Lett. 33 (1992) 4767.
[23] N. Kobayashi, W.A. Nevin, Chem. Lett. (1998) 851.
[24] M.J. Stillman, T. Nyokong, in: C.C. Leznoff, A.B.P. Lever (Eds.), Phthalocyanines-Properties and Applications, vol. 1, VCH, New York, 1989, pp. 133–289.
[25] N. Kobayashi, in: C.C. Leznoff, A.B.P. Lever (Eds.), Phthalocyanines-Properties and Applications, vol. 2, VCH, New York, 1993, pp. 97–161.
[26] N. Kobayashi, H. Konami, in: C.C. Leznoff, A.B.P. Lever (Eds.), Phthalocyanines-Properties and Applications, vol. 4, VCH, New York, 1996, pp. 343–404.
[27] N. Kobayashi, Y. Kobayashi, T. Osa, J. Am. Chem. Soc. 115 (1993) 10994.
[28] (a) H. Akimoto, T. Shioiri, Y. Iitaka, S. Yamada, Tet. Lett. (1968) 97. (b) H. Akimoto, Y. Iitaka, Acta Crystallogr. Sect. B 25 (1969) 1491.
[29] Hemoproteins generally show either positive or negative CD curves throughout both the Soret and Q-band regions, and the shape of which is quite often similar to that of the absorption spectrum. However, the correspondence between the asymmetric environment surrounding the heme and the

sign of the induced CD had not been determined. According to theoretical calculations (M.C. Hsu, R.W. Woody, J. Am. Chem. Soc. 93 (1971) 3515), the induced CD sign was thought to be determined solely by a coupled oscillator interaction between the heme transitions and allowed $\pi-\pi^*$ transitions in nearby aromatic side chains. Therefore, the observation that a Pc having aromatic substituent groups with a right-handed conformer induced negative CD at both the Soret and Q-bands suggested that the asymmetry of a heme environment which shows a negative CD sign is right-handed. Conversely, a heme environment which produced a positive CD sign appeared to be left-handed.

[30] N. Kobayashi, Chem. Commun. (1998) 487.

[31] (a) U.K. Bandarage, J. Simpson, R.A.J. Smith, R.T. Weavers, Tetrahedron 50 (1994) 3463. (b) D. Fabbri, G. Pelogun, O. DeLucchi, J. Org. Chem. 58 (1993) 1748.

[32] N. Kobayashi, R. Higashi, B.C. Titeca, F. Lamote, A. Ceulemans, J. Am. Chem. Soc. 121 (1999) 1208.

[33] W.A. Nevin, W. Liu, S. Greenberg, M.R. Hempstead, M. Melnik, C.C. Leznoff, A.B.P. Lever, Inorg. Chem. 26 (1987) 891.

[34] M.J. Stillman, A.J. Thomson, J. Chem. Soc. Faraday Trans. (1973) 790.

[35] N. Kobayashi, The 62nd Okazaki Conference, January 10–13, 1999, Okazaki, Japan, Abstr. P58.

[36] N. Kobayashi, H. Lam, W.A. Nevin, P. Janda, C.C. Leznoff, T. Koyama, A. Monden, H. Shirai, J. Am. Chem. Soc. 116 (1994) 879.

[37] N. Kobayashi, M. Togashi, T. Osa, K. Ishii, S. Yamauchi, H. Hino, J. Am. Chem. Soc. 118 (1996) 1073.

[38] Y. Kaneko, Y. Nishimura, N. Takane, T. Arai, H. Sakuragi, N. Kobayashi, D. Matsunaga, C. Pac, K. Tokumaru, J. Photochem. Photobiol. A: Chem. 106 (1997) 177.

[39] J.M. Fox, T.J. Katz, S.V. Elshocht, T. Verbiest, M. Kauranen, A. Persoons, T. Thongpanchang, T. Kraus, L. Brus, J. Am. Chem. Soc. 121 (1999) 3453.

[40] J.M. Fox, N.R. Goldberg, T.J. Katz, J. Org. Chem. 63 (1998) 7456.

[41] J.J. Maki, M. Kauranen, A. Persoons, Phys. Rev. Sect. B 51 (1995) 1425.

[42] V.L. Goedken, G. Dessy, C. Ercolani, V. Fares, L. Gastaldi, Inorg. Chem. 24 (1985) 991.

[43] N. Kobayashi, A. Muranaka, K. Ishii, Inorg. Chem. 39 (2000) 2256.

[44] N. Kobayashi, A. Muranaka, Chem. Commun. (2000) 1855.

[45] N. Kobayashi, A. Muranaka, the 50th Annual Meeting of Coordination Chemistry Society, Kusatsu, Japan, September 16–18, 2000.

[46] L.D. Bari, G. Pescitelli, F. Marchetti, P. Salvadori, J. Am. Chem. Soc. 122 (2000) 6395.

[47] C.C. Leznoff, M. Hu, C.R. McArthur, Y. Qin, J.E. van Lier, Can. J. Chem. 72 (1994) 1990.

[48] K. Kasuga, M. Kawashima, K. Asno, T. Sugimori, K. Abe, T. Kikkawa, T. Fujiwara, Chem. Lett. (1996) 867.

[49] (a) N. Kobayashi, The 24th International Symposium on Macrocyclic Chemistry, July 18–23, 1999, Barcelona, Spain, Abstr. OS2-1. (b) F. Narita, Master Thesis, Tohoku University, 1998.

[50] A. Meller, A. Ossko, Monatsh. Chem. 103 (1972) 150.

[51] H. Kietaibl, Monatsh. Chem. 105 (1974) 405.

[52] C.G. Claessens, T. Torres, Eur. J. Org. Chem. (2000) 1603.

[53] C.G. Claessens, T. Torres, Chem. Eur. J. 6 (2000) 2168.

[54] T. Nonomura, N. Kobayashi, unpublished results.

[55] C.S. Velazquez, W.E. Broderick, M. Sabat, A.G.M. Barrett, B.M. Hoffman, J. Am. Chem. Soc. 112 (1990) 7408.

[56] J.W. Sibelt, S.J. Lange, C.L. Stern, A.G. Barrett, B.M. Hoffman, Angew. Chem. Int. Ed. Engl. 34 (1995) 2020.

[57] K. Anderson, M. Anderson, O.P. Anderson, S. Baum, T.F. Baumann, L.S. Beall, W.E. Broderick, A.S. Cook, D.M. Eichhorn, D. Goldberg, H. Hope, W. Jarrell, S.G. Lange, Q.J. McCubbin, N.S. Mani, T. Miller, A.G. Montalban, M.S. Rodriguez-Morgade, S. Lee, H. Nie, M.M. Olmstead, M. Sabat, J.W. Sibelt, S. Stern, A.J.P. White, D.G.B. Williams, D.J. Williams, A.G.M. Barrett, B.M. Hoffman, J. Heterocycl. Chem. 35 (1998) 1013.